J Appl Electrochem (2014) 44:509–522
DOI 10.1007/s10800-013-0640-4

RESEARCH ARTICLE

Electrical double-layer capacitors: evaluation of ageing phenomena during cycle life testing

Noshin Omar · Hamid Gualous · Justin Salminen · Grietus Mulder · Ahmadou Samba · Yousef Firouz · Mohamed Abdel Monem · Peter Van den Bossche · Joeri Van Mierlo

Received: 23 July 2013 / Accepted: 15 October 2013 / Published online: 26 October 2013

Abstract This paper represents an assessment of the main ageing phenomena in electrical double-layer capacitors (EDLCs). In this study the cycle life of the EDLC cells with a rated capacitance of 1,600 F has been investigated at different ambient temperatures and current rates. From the experimental results we can observe that the impact of the high ambient temperature is significant on the cycle life of the cells. Moreover, the results also show the negative impact of the current rate. The internal resistance tests showed that the increase of the resistance is much higher than the decrease of the capacitance. Thus, the ageing of the EDLC during cycling was clearly non-linear. Further the EIS measurements indicated the higher increase of the imaginary part of the impedance at low frequencies during cycling, which indicates the capacitance fade.

Keywords Electrical double-layer capacitors · Ageing · Internal resistance increase · Capacitance fade · EIS · Lifetime model

N. Omar (✉) · G. Mulder · A. Samba · Y. Firouz · M. A. Monem · P. Van den Bossche · J. Van Mierlo
Vrije Universiteit Brussel, Pleinlaan 2, 1050 Brussels, Belgium
e-mail: noshomar@vub.ac.be

H. Gualous · A. Samba
LUSAC, Université de Caen Basse Normandie, Rue Louis Aragon, BP 78, 50130 Cherbourg-Octeville, France

J. Salminen
Technical Research Centre, Espoo, Finland

G. Mulder · M. A. Monem
VITO, Unit of Energy Technology, Boeretang 200, 2400 Mol, Belgium

1 Introduction

Due to increase of the gas prices and environmental concerns, battery electric vehicles (BEVs) have recently drawn more attention. In BEV configurations, electrical energy storage is a key issue in the design of these vehicles [1–3]. Presently batteries are used in most applications as energy storage devices. The batteries should be sized to meet the energy and power requirements of the vehicle. However, in many hybrid applications the power required is sufficiently high that the battery is sized by power, which results that a battery pack in these vehicles is often over dimensioned [4–6]. Hereby, the optimal use of the energy becomes very difficult [4]. These shortcomings could be solved by the implementation of a hybrid topology [7–11].

A hybrid electric vehicle topology (HEV), consisting of a high energy density source such as a battery pack and other high power density source [like electrical double layer capacitor (EDLC)], offers a compromise [11–13]. It allows batteries to extend service life, to minimize batteries losses, to achieve efficient energy recuperation and extended autonomy [14]. EDLCs are very convenient energy storage systems for applications where high power is needed.

In the last decade, EDLCs have received a considerable attention in heavy-duty applications such as buses, trams and metros [7–25], and more in particular for city buses, where the driving cycles are very heavy due to the traffic and congestion conditions. The internal combustion engine (ICE) is often operating in a low energy efficiency region. From the Belgium context, Barrero et al. [16] concluded that 32–40 % fuel saving can be achieved by hybridization of the diesel-electric MERCEDES CITO buses with EDLCs and with an associated converter. The obtained results of fuel saving are due to recovery of the braking energy and

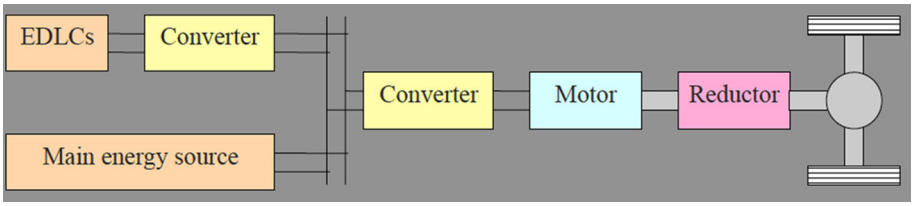

Fig. 1 Overview of the driveline in hybrid electric vehicle

due to a more efficient use of the ICE. This analysis has been done based on an advanced simulation model.

According to the bus manufacturer Van Hool, the series hybrid buses (ICE+EDLCs) as presented in Fig. 1 consume 30 % less fuel [26]. This leads to a reduction of CO_2 emissions of the bus. The fuel consumption decrease in the hybrid bus fleets featuring SCANIA buses in Stockholm and MAN buses in Neurenburg is in the range of 20–25 % [27–30].

In [31] the authors documented that implementation of EDLCs in the Brussels metro network can result in energy saving up to 36.4 %. This value for energy saving also has been approved by Bombardier [32]. They concluded that EDLCs have a high impact on the reduction of the line voltage drop (up to 50 %) during acceleration [32]. In 2002, Siemens started in Madrid with the establishment of stationary energy storage systems (SESS) which is called SITRAS (Energy Storage System for Mass Transit Systems) [32, 33]. This system uses EDLCs for the stabilization of the line voltage of metros between 490 and 520 V [28, 30]. During acceleration, SESS provides the electric power to the vehicles and during braking the kinetic energy can be stored back in the SESS. Due to the SESS the overall performance and reliability of the system can be enhanced and the energy efficiency can be improved. According to measurements, the above-described system is able to save energy up to 30 % [27, 32].

But, the success of EDLCs was not only limited to heavy duty vehicles. In [8, 10, 15, 17, 19, 34–39] a series of applications are reported where the EDLCs have approved their suitability. In extreme cold conditions, a lead–acid battery is not able to start the diesel fuelled ICE at temperature around −20 °C [39]. Due to the wide operating range, the hybridization of lead–acid battery with EDLCs can be of high importance. Nowadays, uninterruptible power supply systems (UPS) use batteries more for small applications but also a generator set is one of the possibilities for large systems [39]. However all these energy storage systems have their limitations. In order to overcome this problem, EDLCs may be a good solution for small applications and in combination with other sources such as lead–acid batteries for large systems. Furthermore EDLCs have been implemented in many other applications such as in wind turbines, elevators and portable applications [35–39]. Particularly in the case of public elevators, the EDLCs could be of high importance during up movement where considerable high energy can be recuperated and provided during down movement of the elevator.

However, in all these applications, the lifetime of EDLCs is one of the major critical parameter. Since the cost of the EDLCs is relatively high (0.1€/F) [40], from the application point of view, it is required to have a long lifetime as illustrated in Table 1.

In the most applications, a cycle life of 1,000,000 cycles or higher is desired. However, this value is strongly depending of the operating conditions of the EDLCs.

During the last decade, significant research work has been carried out regarding the evaluation of the lifetime performances of EDLCs at different working conditions [41–51].

In Chaari et al. [41] investigated the aging phenomena in EDLCs by applying a HEV cycle at two different voltage levels (2.7 and 2.5 V). They concluded that the impact of the higher voltage has a negative impact on the EDLC cycle life. They observed a reduction of cycle life by factor two when the operating voltage is higher than 200 mV.

Following to this work, Hammar et al. [42] carried out similar analysis, whereby the EDLCs have been cycled based on a current load profile, which is representative for railway applications.

In Uno et al. [43] cycled the EDLCs during charging and discharging. The aim of this study was to establish a cycle life model. However, in this work the Arrhenius law has been applied for determining the cycle life at another temperature.

In Betrand et al. [44] and Coquery et al. [45] cycled the EDLCs based on a HEV load profile. All these work have shown that the impact of the working temperature and the voltage level aaffect significantly the EDLC long term capabilities. This conclusion also has been confirmed by Kötz et al.; Oukaour et al. and Gualous et al. [46–48]. In [49–51] it is reported that the negative impact of the high voltage on the EDLC lifetime is related to occurrence of the redox reactions, which are favored because of the presence of impurities in the electrodes and in the electrolytes. This leads that the electrolytes degradation accelerates. Regarding higher working temperatures, the reactivity of the chemical reactants in the EDLCs

Table 1 Application requirements

Application	Voltage (V)	Power (W)	Lifetime	Operating sequence
Bus	700–800	100 k	1000.000 cycles	10 s
Metros	800–900	1–2 M	200.000–400.000 cycles/year	10–20 s
Trams	700	300–400 k	?	10–20 s
Load levelling	400	200 k–1 G	2500/10 years	60–300 min
Back-up power	400	1 k–1 M	100/10 years	15 min
Cranes	800	350 k	1000.000 cycles	10 s

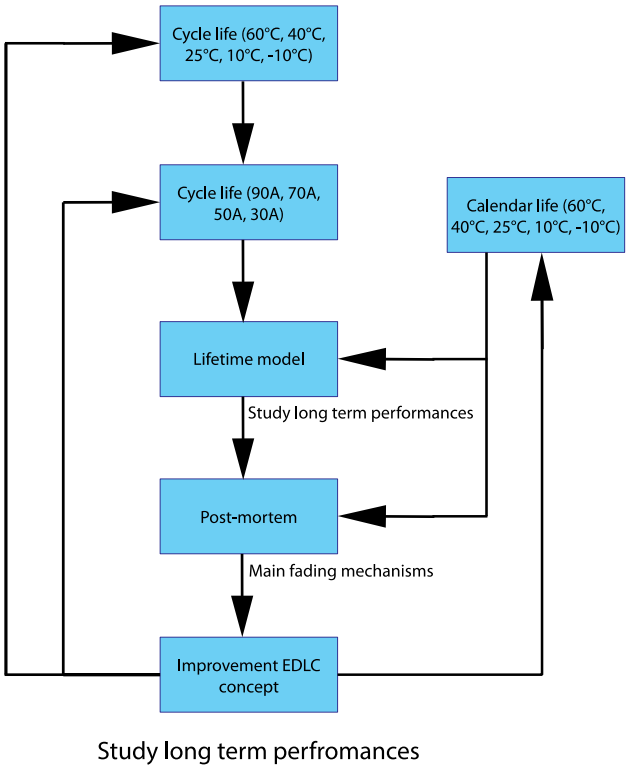

Fig. 2 Test methodology

increases. However, under such conditions overvoltage and structural changes can occur on the electrode level, which will accelerates the degradation in the EDLC.

However, all these studies were limited in terms of operating conditions of the EDLCs, which do not reflect the complete operating window of the EDLC. Further, most of the existing works are based on accelerated conditions, such as high ambient temperatures, high current rates or high voltages. In this paper, an extended analysis has been carried out at different ambient temperatures and current rates. The extraction of the cycle life versus ambient temperature, current rates and calendar life will provide us the required information for the establishment of a general lifetime model for EDLCs. Furthermore, this investigation will assist us to evaluate the main changing parameters during cycle for the development of a state-of-health prediction technique.

2 Methodology

In Fig. 2, the test methodology is presented that has been applied in this study. As we can observe the lifetime investigation of EDLCs has been performed at different working conditions such as:

- Ambient temperatures (60, 40, 25, 10 and −10 °C),
- Current rates (90, 70, 50 and 30 A),
- Calendar life (60, 40, 25, 10 and −10 °C),

As it is illustrated, the proposed test methodology will allow us to obtain the cycle life relationships versus the mentioned working conditions for development of a cycle life model for EDLCs. Moreover, this analysis will assist us to evaluate the main ageing parameters of the EDLCs. Finally, the EDLCs, will undergo post-morten when the capacity has been decreased till 20 % or the internal resistance is increased with 100 %. The analysis of the post-mortem will provide us additional information regarding the physical degradation phenomena on a material level (electrode surface change, gas evolution inside the cell, electrolyte decomposition, separator structural change).

Here, it should be noted that only the experimental results (capacitance, resistance, power evolutions) at 90 and 70 A and at the above-mentioned ambient temperatures are demonstrated.

In this paper, the EDLC cells of NESSCAP ESHSR-1600C0-002R7A5 (1600F) have been used for this investigation [52].

In order to investigate all the performance parameters such as internal resistance, capacitance, temperature and impact of frequency, the battery tester SBT 0550 from PEC company and the impedance spectroscopy from Bio-Logic HCP-1500 have been used [53, 54]. In order to keep the cells at the mentioned ambient temperature, a number of climate chambers have been used, whereby the ambient temperature has been set up.

Here it should be underlined that calendar life test are not included in this article. The analysis based on calendar life test will be investigated in a separate article.

In order to assess the cycle life of EDLCs, the test sequence as presented by Fig. 3 has been used. As we can

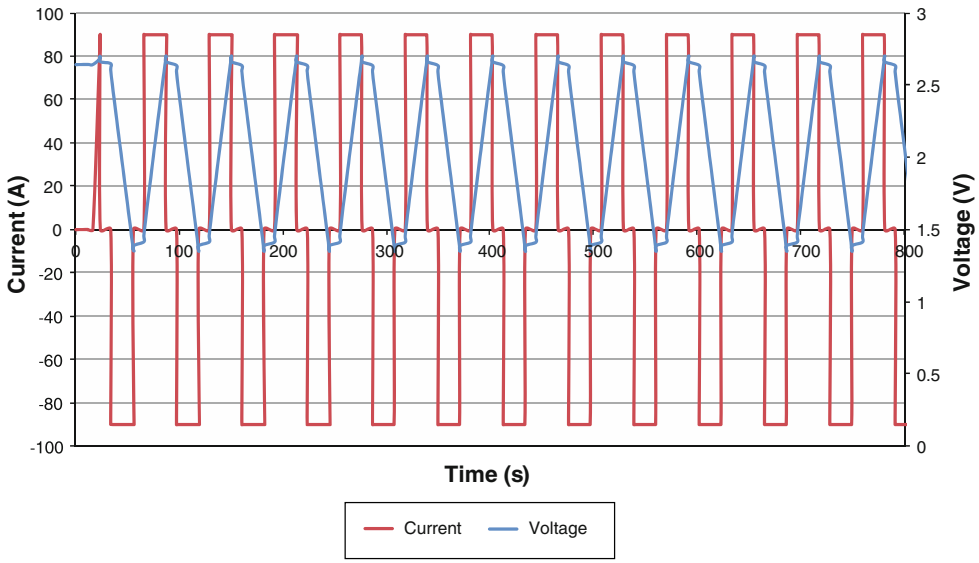

Fig. 3 An example of the test sequence cycling at 90 A

observe the EDLC cells have been cycled between U_{max} (2.7 V) and $U_{max/2}$ (1.35 V). The rest time between charging and discharging is 5 s.

The reason for selection of these voltage levels is related to the energy that can be obtained from the EDLCs. For optimal usage of an EDLC as a peak power unit, the voltage of the EDLC should not be kept constant. Normally an EDLC voltage ranges from 100 to 50 % of its nominal voltage to keep an acceptable efficiency of the energy transfer. According to Eq. (1), we can conclude that the EDLC system can release 75 % of the energy content when the voltage over the system is discharged from a maximum voltage of U_{max} to $U_{max/2}$, which can be performed by using a bidirectional DC–DC converter as presented by Fig. 1.

$$E = \frac{1}{2} \cdot C. \left(U_{max}^2 - U_{max/2}^2 \right) \quad (1)$$

where E the energy (J), C the capacitance (F), U_{max} the maximum voltage (V) and $U_{max/2}$ half of the maximum voltage (V).

In order to assess the degradation of all EDLCs cells, at every 10,000 cycles the cells have been characterized at 25 °C based on capacitance and resistance checks and at every 30,000 cycles EIS measurements have been performed.

3 Results and discussions

3.1 Capacitance

In Fig. 4 the capacitance evolution of the EDLCs is illustrated at different ambient temperatures and current rates. The capacitance has been determined based on the methodology as described in the standard IEC 62576, whereby the cells have been charged until the maximum voltage (2.7 V). Then after a rest period of 10 min the cells have been discharged at 10 A until 0.3 V. Prior starting, the EDLCs have been placed in the climate chamber for a period of 6 h at the specified ambient temperature (50 % humidity).

The capacitance has been calculated between U_1 and U_2 as illustrated in Fig. 5 and presented by Eq. (2).

$$C = I \frac{t_2 - t_1}{U_1 - U_2} \quad (2)$$

where $U_1 = 80$ %. U_{max} (V), $U_2 = 40$ %.U_{max} (V), t_1 the time at U_1 (s), $t_2$the time at U_2 (s) and I the current (A).

In Fig. 4, the capacitance check evolution during cycle life is illustrated at 25 °C ambient temperature. The tests have been carried out at 10 A charging until 2.7 V and after 5 min the EDLCs have been discharged till 0 V at 10 A. Based on the voltage and time evolutions (between 80 and 40 % of the rated voltage of the EDLC: 2.7 V) and imposed current, the capacitance of the examined EDLCs have been determined according to Eq. (2).

From Fig. 4, we can conclude that the decrease of the capacitance is significant at high ambient temperatures of 60 and 40 °C compared to 25, 10 and −10 °C. Here we can observe that between 0 and 10,000 cycles the capacitance fade is relatively high, while from 10,000 cycles and forward the capacitance fade is almost linear. This evolution is also similar to lithium-ion batteries [56].

The end of life of EDLCs criterion is based on the reduction of the capacitance by 20 % or the increase of the internal resistance by 100 % [57]. According to the experimental results, the cycle life of the EDLC cells at ambient temperature 60 °C and cycling at 90 A is 110,000 cycles. Cycling the EDLC at 40, 25, 10, −10 °C and 90 A, the capacitance degradation is 10.2, 7.2, 4.1, 6.1 %,

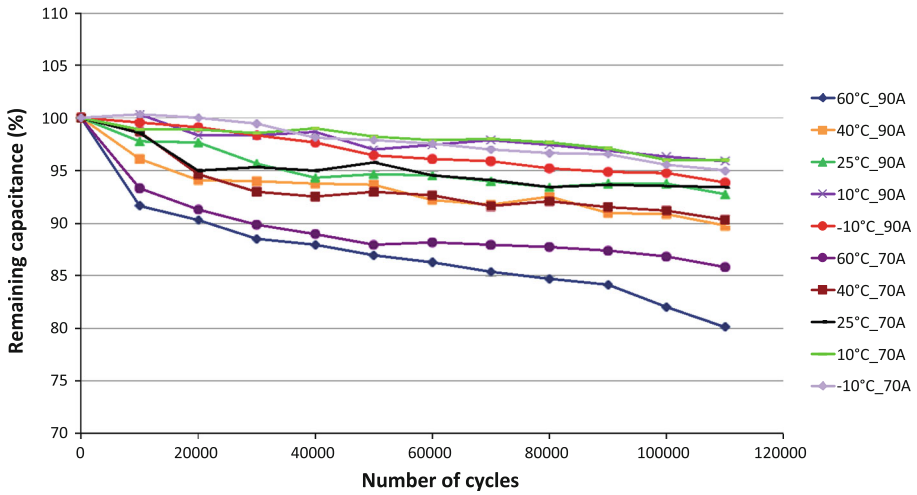

Fig. 4 Capacitance check evolution as function of number of cycles at 25 °C ambient temperature for the EDLCs during cycling at the mentioned currents and ambient temperatures

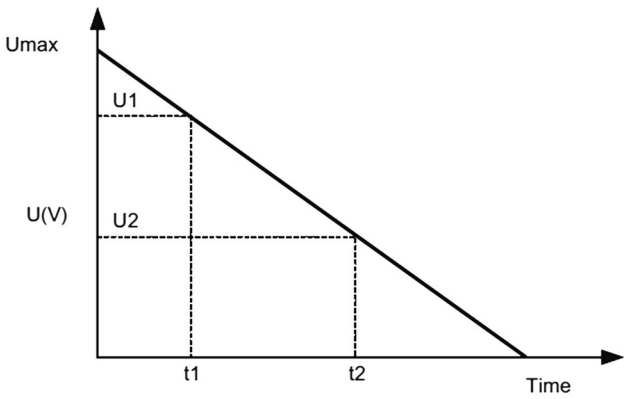

Fig. 5 Test methodology for determining the capacitance of the EDLC cell based on the standard IEC 62576 [55]

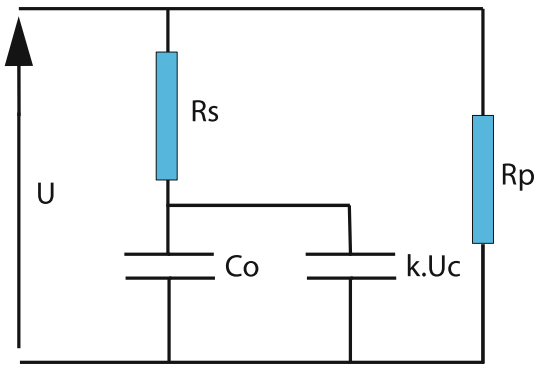

Fig. 6 EDLC model [61]

respectively. Thus, the capacitance fade of the EDLC is higher at higher ambient temperatures.

In Fig. 4, we can recognize that the applied current rate has an impact on the EDLC capacitance fade. Particularly at 60 °C and 70 A cycling the capacitance fade is less than at 90 A cycling. These results can be explained due to the smaller heat generation in the cell.

At other ambient temperatures, the differences between 70 and 90 A cycling are quite small (max. 1 %).

In [46] is reported that the accelerated capacitance fade at high temperature is attributed to the decomposition of the electrolyte, which produces gases into the cell and thus increases the pressure in the cell, whereby the mechanical stress increases [58] (generation of H_2 in the case of acetonitrile or CO_2 in the case of propylene carbonate [59]).

Then, such a process leads to oxidation of the surface of the carbon electrode and further the closing of the pores access to the ionic depletion in the electrode [58].

In Brouji et al. [60], ascertain that the capacitance degradation during cycling is also contributed to the decomposition of impurities such as water. The formation of these parasitic reactions is captured in the pores of the activated carbon, which is limiting the access of ions to the porous structure.

From this context, we can conclude that the control strategy of the thermal management of the EDLC should avoid high temperatures during operating conditions.

Furthermore, in Fig. 4, we can observe that the impact of the current 70 A on the cycle life is almost identical with 90 A cycling and at the ambient temperatures 40, 25, 10 and −10 °C.

Here it should be noted that the general objective of 1,000,000 cycles cannot be achieved for the investigated EDLC cell.

If we extrapolate the obtained value at 25 °C, the end of life of the investigated EDLC cell will be reached around 300,000 cycles. However, it should be noted that the extrapolation cannot be used, since the capacitance fade between 0 and 10,000 cycles is relatively higher than from 10,000 cycles and forward.

Furthermore, one can conclude that the EDLC model as presented in Fig. 6 is not able to predict the EDLC long-term performances, accurately. The model proposes that the parameter C_o, which represents the initial capacitance,

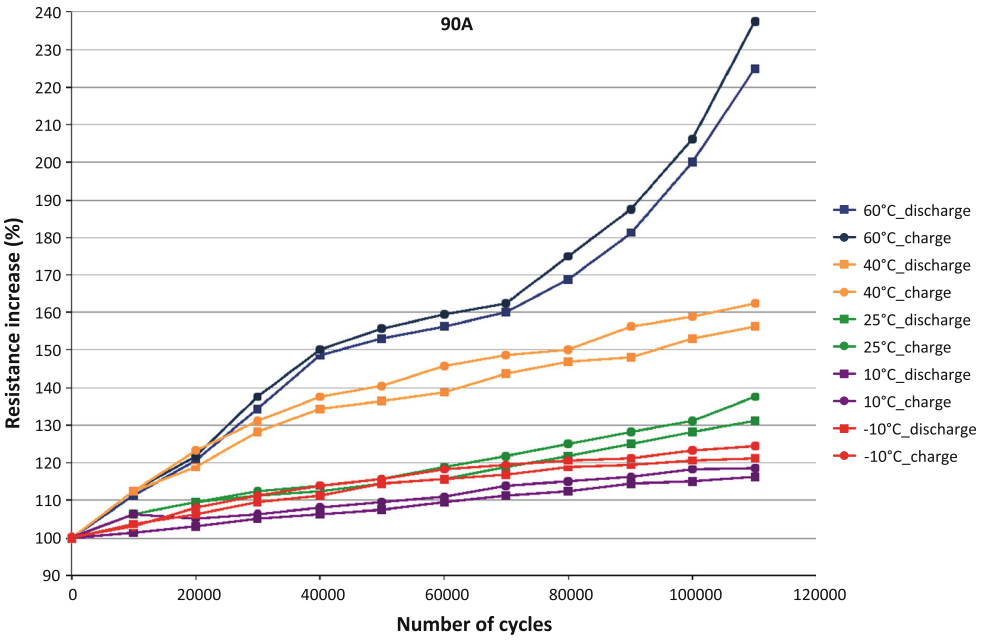

Fig. 7 Evolution of resistance versus number of cycles and ambient temperature at 90 A cycling

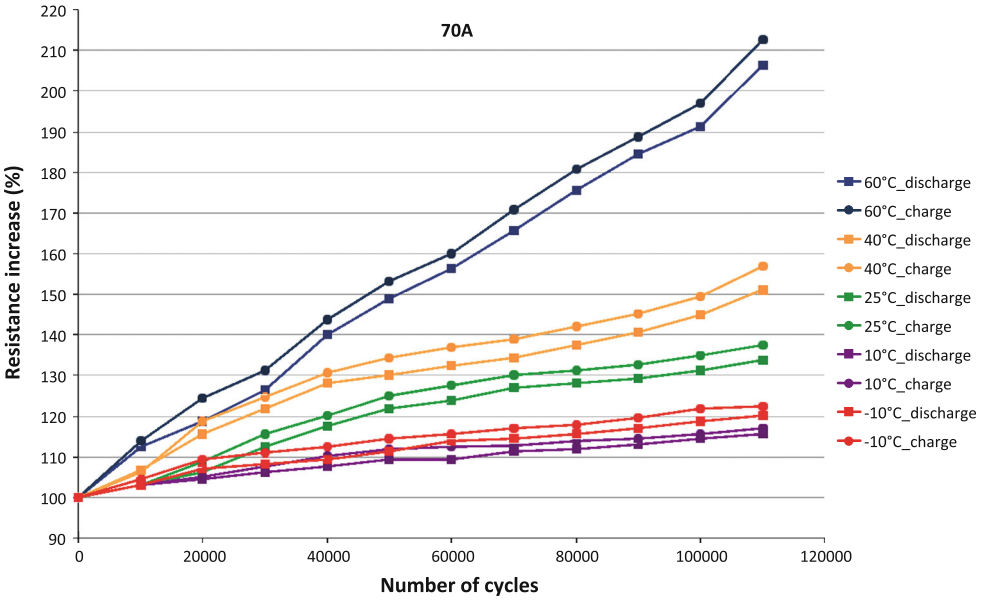

Fig. 8 Evolution of resistance versus number of cycles and ambient temperature at 70 A cycling

is a constant parameter and the parameter k. U_c corresponds to the voltage dependent capacitor, which varies linearly with the voltage.

However, the capacitance of the EDLCs decreases as we observed in Fig. 4. Then, the capacitance is changing significantly as function of working temperature and less as function of current rate.

3.2 Resistance

In Figs. 7 and 8, the evolution of the internal resistance of the EDLC cells at different ambient temperatures and 90 and 70 A, respectively are illustrated.

The resistance has been calculated based on the methodology as described in the standard IEC 62576 and demonstrated in Fig. 9. The EDLC cells have been charged at 10 A and after 10 min rest, they have been discharged at 30 A till $U_{max/2}$ has been reached. Then, the cells are rested for 10 min rest and have been charged at the same current rate (30 A).

The resistance has been determined based on the Eq. (3):

$$ESR = \frac{\Delta U_3}{I} \tag{3}$$

In Fig. 7, we can recognize the increase of the internal resistance of the EDLC cells at the different ambient

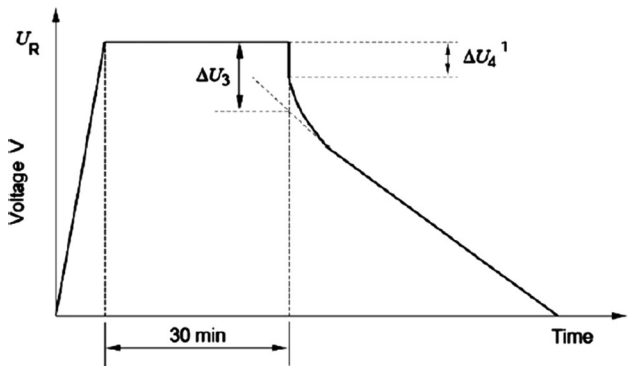

Fig. 9 Determining of the resistance of the EDLC according to the standard IEC 62576 [53]

temperatures. However, the highest increase can be observed at 60 °C, whereby the increase after 110,000 cycles at 90 A cycling is 125 % compared to 106 % at 70A cycling. Here we can conclude that the increase of the internal resistance is much faster than the decrease of the capacitance, which leads to the fact that the cycle life of the investigated EDLC at 60 °C and 90 A cycling is not 110,000 cycles as we concluded in the Sect. 3.1. But the cycle life is 100,000 cycles. In Fig. 7 one can observe the high increase of the internal resistance from 70,000 cycles and forward.

At 40, 25, 10 and −10 °C, the increase of the resistance is clearly temperature dependent and is 56, 31, 16 and 21 %, respectively. Based on Figs. 7 and 8, the evolution of the resistance at all ambient temperatures with exception at 60 °C, is almost linear. This result makes the calculation of the end of life of the EDLC easier by using the linear extrapolation method.

Furthermore, when we compare Fig. 7 against Fig. 8, we can conclude that the increase of the internal resistance at the same ambient temperature is less pronounced at 70 A, where the increase of the resistance after 110,000 cycles, is 106, 51, 33, 15 and 20 %, at 60, 40, 25, 10 and −10 °C, respectively.

Here it should be noted that the applied current rate has three major impacts on the performances of the EDLCs.

1. At 90 A, the generated heat ($R \cdot I^2$) is higher than at 70 A during cycling, whereby the acceleration of the decomposition of the electrolyte (tetraethylammonium tetrafluoroborate, $(C_2H_5)_4N^+$ BF_4^- in acetonitrile, CH_3CN) is faster as reported by Hahn et al. [59] and Zhu et al. [62].
   Brouji et al. [60] concluded that during cycling the increase of the electrolyte resistance is significant compared to calendar tests. The increase of the electrolyte resistance has been related to the diminution of the pores diameters, which leads to a reduction of the ions mobility.
   In Figs. 10 and 11, the surface temperature of the EDLC cells has been measured at 10 and 40 °C and at 70 and 90 A. As it is illustrated the increase of the surface temperature at 10 °C after 110,000 cycles is 3 and 7.4 °C at 70 and 90 A, respectively. While the increase of the surface temperature at 40 °C is 4 °C at 70 and 8 °C at 90 A. Here it should be noted that the increase of the surface temperature is limited due to the implemented rest time between charging and discharging and vice versa (5 s).
2. Since the maximum temperature is higher at 90 A cycling then the gas development in the cell is more pronounced [49, 50].
3. Therefore, one can expect more synthesis and deposition of unwanted substances on the electrode surface [58, 59]. Hereby the active elements in the systems undergo irreversible process, whereby this influences the capacitance and the internal resistance [61, 62].

All these 3 process are similar to the electrochemical solid interface in most lithium-ion based batteries. Thus, the ageing phenomena in EDLCs cannot be generalized. Since most existing work regarding ageing of EDLCs is based on calendar tests, there is a need to perform a similar analysis on aged tests during cycling.

Furthermore, based on the Figs. 7 and 8, we can conclude that the higher increase of the resistance at higher ambient temperatures (60 and 40 °C) leads to fact that the energy efficiency decreases and the heat generation in the EDLC will be high. Therefore, it is required to have a dedicated thermal management strategy to remove the heat from the EDLC cells or pack. However, the size of the cooling system is here of high importance. Therefore, the cooling system should be designed based on the worst-case scenario and it should not be based on the scenario at the beginning of life.

In order to guarantee a long cycle life and high performances, the control strategy of the thermal management should avoid operating temperatures above 40 °C. Thus, the role of the thermal modeling can be of high importance.

In peak power applications such as hybrid electric vehicles, the EDLCs should supply at every moment the required power during acceleration and braking events. However, the power evolution during cycling as presented in Figs. 12 and 13 show that the power performances of the investigated EDLCs are varying significantly during cycle life. As we can observe the power performances of EDLCs reduces the more the ambient temperature increases with exception at 10 °C. This evolution is related to the increase of the internal resistance at these temperatures. Here, we can conclude that cycling the EDLCs at 60 °C will not only have a negative impact on the thermal behaviour and energy efficiency, but it influences in the negative sense the power capabilities likewise. Regarding ageing, we can recognize that the impact of

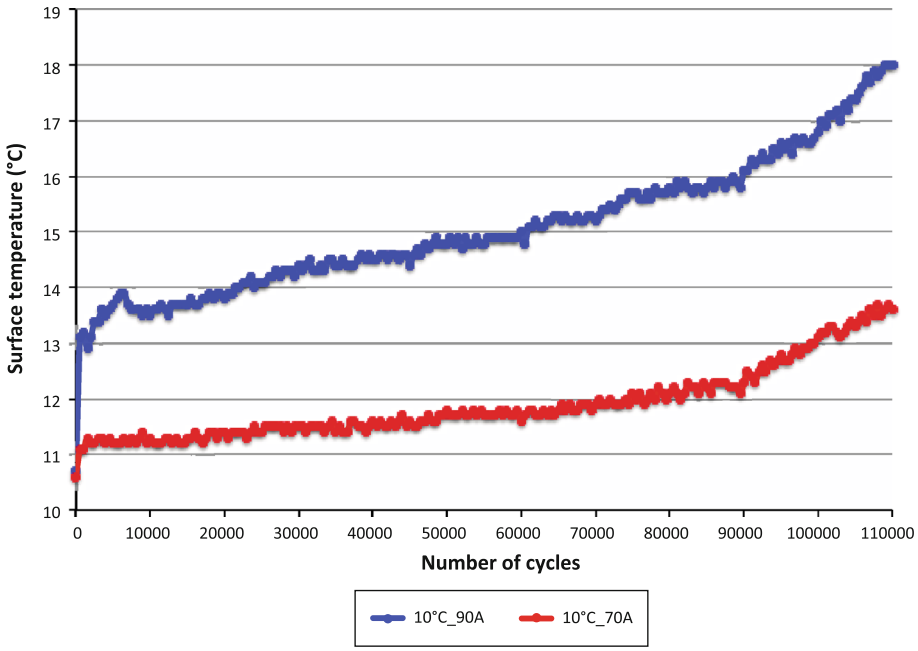

Fig. 10 Evolution of the surface temperature versus number of cycles at 10 °C

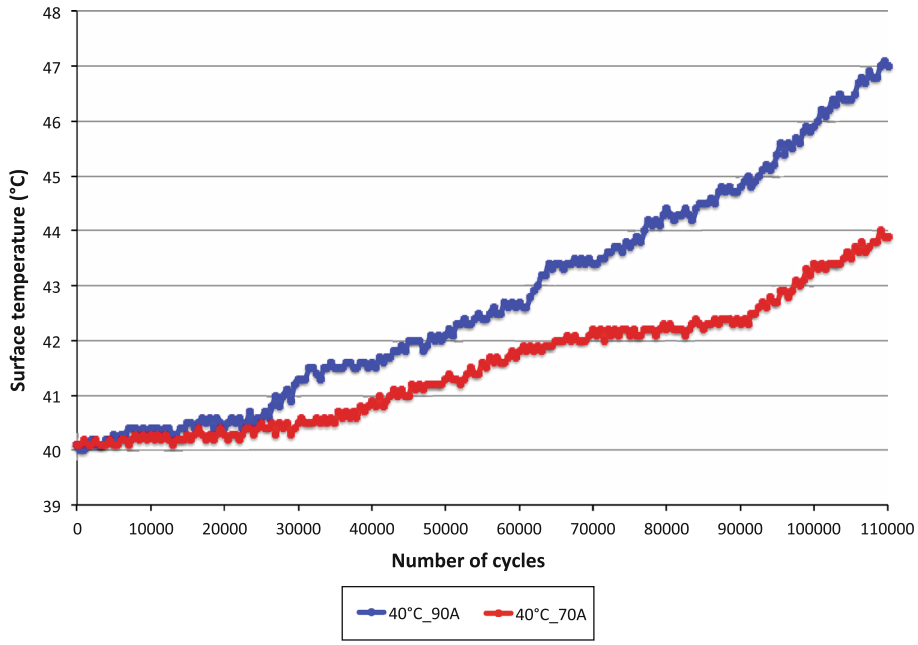

Fig. 11 Evolution of the surface temperature versus number of cycles at 40 °C

cycling at 70 A against 90 A is less pronounced at the ambient temperatures (40, 25, 10 and −10 °C).

Here it should be noted that the power has been calculated as proposed by the standard (see Eq. 4) [55]:

$$P = \frac{U^2}{4 \cdot R} \tag{4}$$

where P the power (W), U the nominal voltage (V) and R the resistance as determined based on the standard IEC 62576 method (Ω).

As emerging result from the other studies, based on the evolution of the internal resistance in the Figs. 7 and 8, we can conclude that the hysteresis of EDLC clearly exists. As one can see, the hysteresis is strongly temperature dependent as in lithium–ion batteries.

In [63] it is documented that during ageing, the anode positive electrode is more affected than the negative electrode. In addition, they concluded that this is due to the specific area and pore volume change of the aged positive electrode. In addition, they observed that large micropores

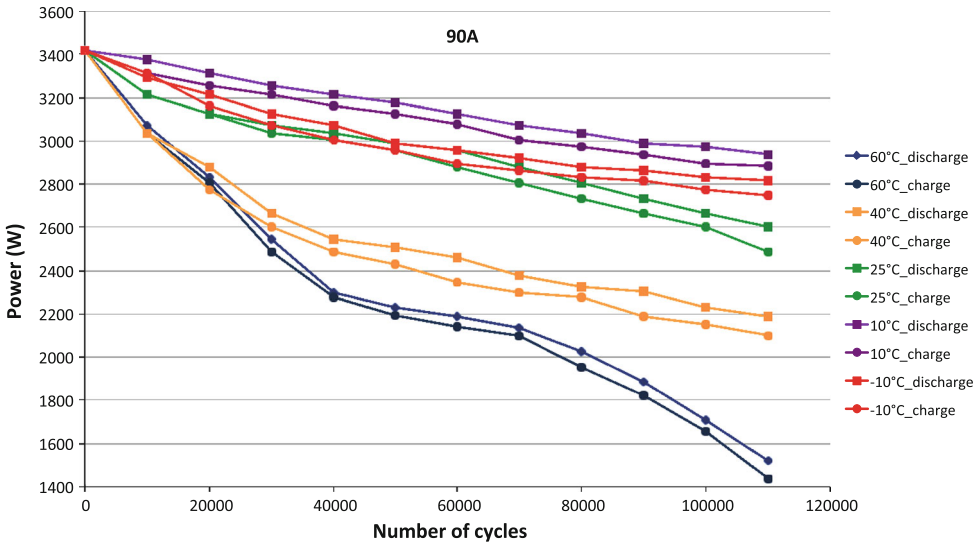

Fig. 12 Charge and discharge power performances during cycling and 90 A and different ambient temperatures

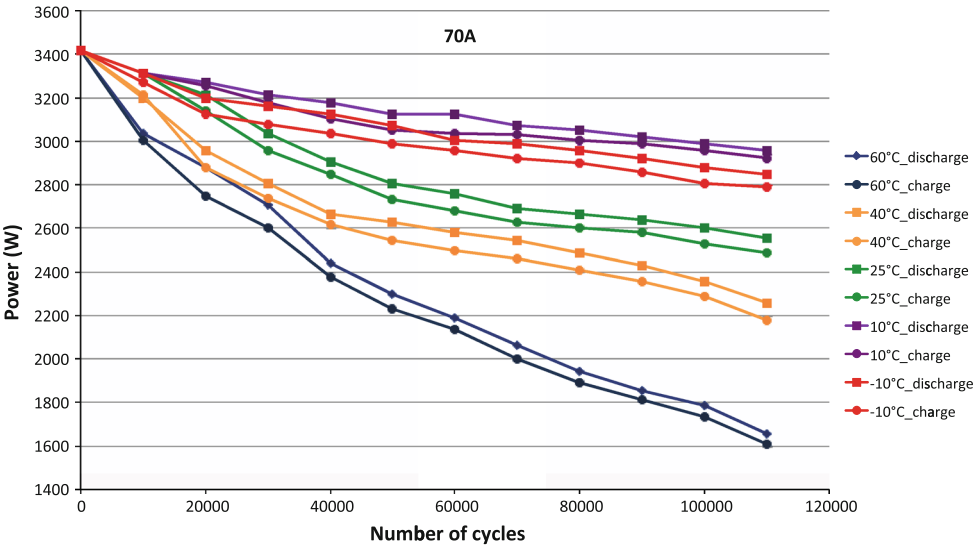

Fig. 13 Charge and discharge power performances during cycling and 70 A and different ambient temperatures

(1.26–2 nm) and small mesopores (2–3.2 nm) are blocking by polymerized solvent acetonitrile.

3.3 EIS analysis

In order to study the behaviour of the aged EDLCs in depth, a number of electrochemical impedance spectroscopy measurements have been carried out. The measurements have been conducted with the potentiostat EIS device, Bio-Logic HCP-1500, at every 30,000 cycles and at 100 % SoC. 100 % SoC corresponds to a voltage of 2.7 V. The EIS tests have been started after a rest period of 30 min.

In order to compare the results of all the cells, the tests have been done at 25 °C. In this paper, the frequency range between 10 and 50 mHz has been selected, which is in accordance with the time constant of the most power applications.

From Figs. 14, 15, 16, 17 and 18, we observe a shift of the spectra along the real axis during cycling at different ambient temperatures. The shift of the spectra corresponds to the increase of the ohmic resistance of the EDLC cells. In this context, we see a similar evolution to the resistance measurements as in Sect. 3.2. However, the increase of the ohmic resistance based on EIS measurements is much higher as illustrated e.g. in Fig. 14. The increase of the ohmic resistance at ambient temperature 60 °C and cycling at 90 A after 90,000 cycles is 300 % compared to about 230 % based on the method as described in the standard IEC 62576. However, the increase of the ohmic resistance at 40, 25, 10 °C and −10 °C at 90A cycling and after 90,000 cycles is 200, 80, 50 and 220 %.

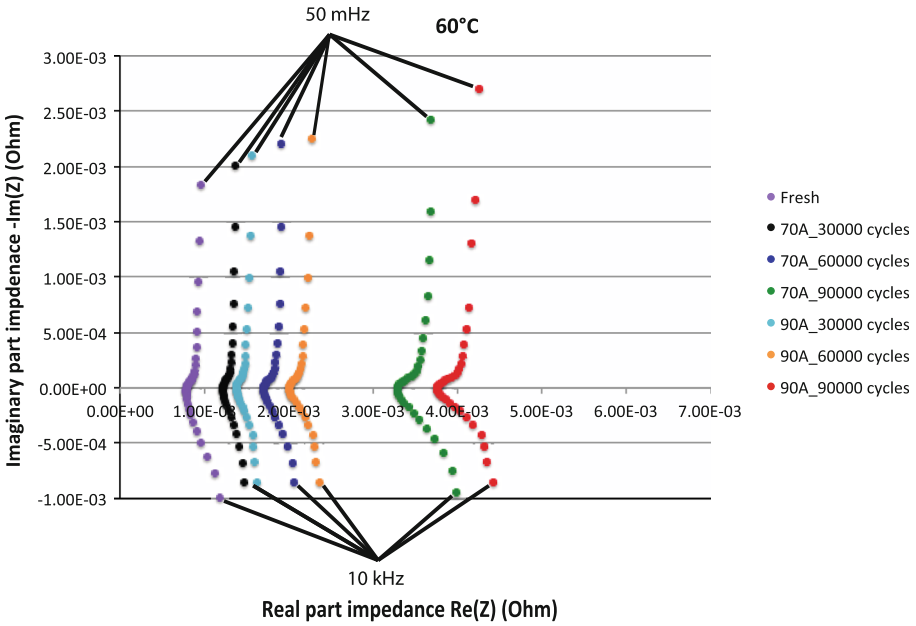

Fig. 14 Effect of the cycle life on the impedance spectra at 60 °C in a Nyquist plot

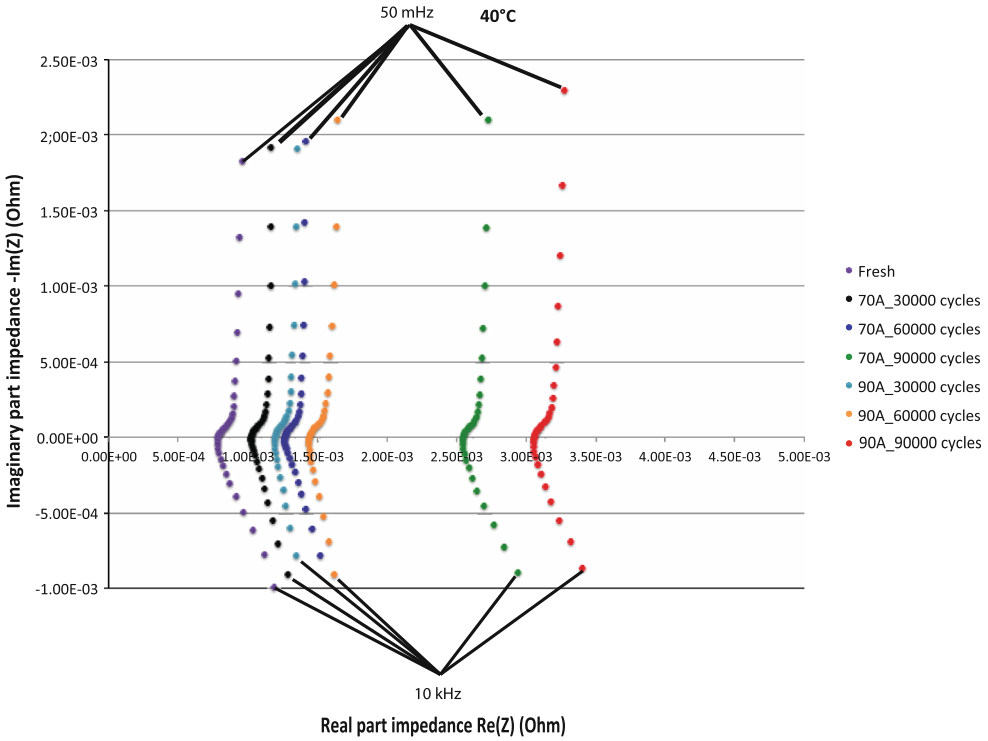

Fig. 15 Effect of the cycle life on the impedance spectra at 40 °C in a Nyquist plot

In Figs. 14, 15, 16, 17 and 18, we recognize that the increase of the resistance during cycling is not linear. Particularly, this evolution is noticeable at 60, 40 and 25 °C where, the increase of the ohmic resistance is higher between 60,000 and 90,000 cycles against between 30,000 and 60,000 cycles as we concluded in Sects. 3.1 and 3.2. This means that the ageing of the EDLCs during cycling is non-linear.

By comparing the experimental results in the Figs. 14, 15, 16, 17 and 18, we can notice that the imaginary part of the resistance at low frequency also increases during cycling. This result indicates that the capacitance of the EDLC decreases, which is in accordance with the Eq. (5):

$$\mathrm{Im}(Z) = -\frac{1}{2 \cdot \pi \cdot f \cdot C(f)} \tag{5}$$

where Im(Z) the imaginary pary of the impedance (Ω), f the frequency (Hz) and C the capacitance of the EDLC (F).

In [64, 65] it is reported that the capacitance behavior is strongly dependent on the capacitive surface position in the

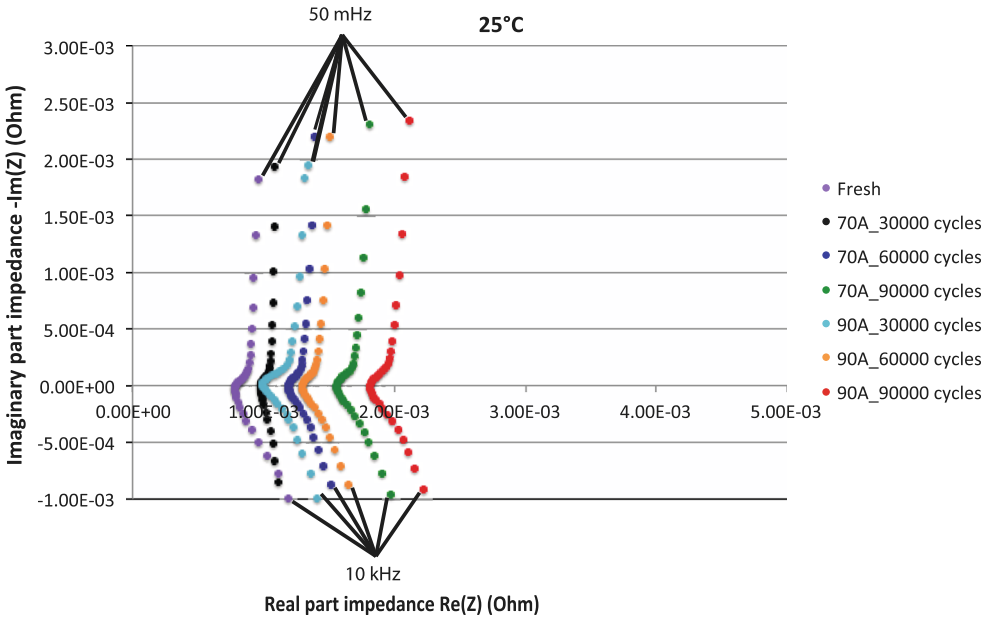

Fig. 16 Effect of the cycle life on the impedance spectra at 25 °C in a Nyquist plot

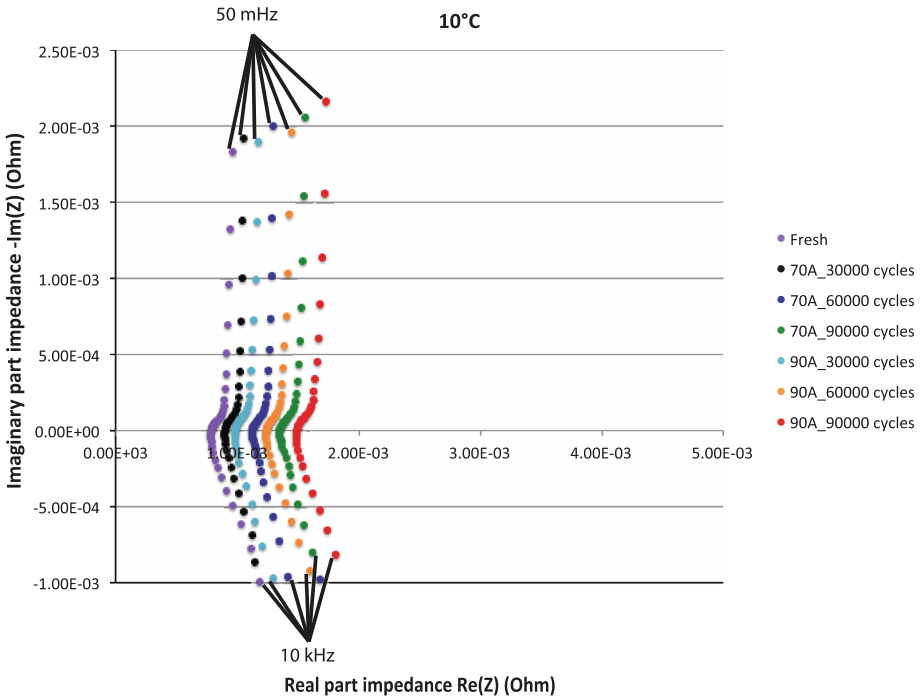

Fig. 17 Effect of the cycle life on the impedance spectra at 10 °C in a Nyquist plot

positive electrode. If the surface considered lays deep into a carbon pore, the access time for the ions to this surface will be longer than for an external pore surface.

The evolution of the experimental result has also been documented by the references [46, 48, 58–60, 66]. Following to the obtained results and latter works, we can conclude that the EDLCs during cycling behave capacitive.

Following the conclusions, we observe in the Figs. 14, 15, 16, 17 and 18 that the shift of the spectra along the real axis at 70 A cycling is smaller than at 90 A. This indicates that higher current rates accelerate the ageing phenomena in the EDLCs. Then, the results also demonstrate that the increase of the imaginary part is smaller against cycling at 90 A.

Thus, here we can conclude that the assessment of a lifetime model for EDLC is complicated and dependent on many parameters.

3.4 New EDLC model approach

In Sect. 3.1 (Fig. 6), we have seen a popular EDLC model. The model has been developed based on fixed parameters.

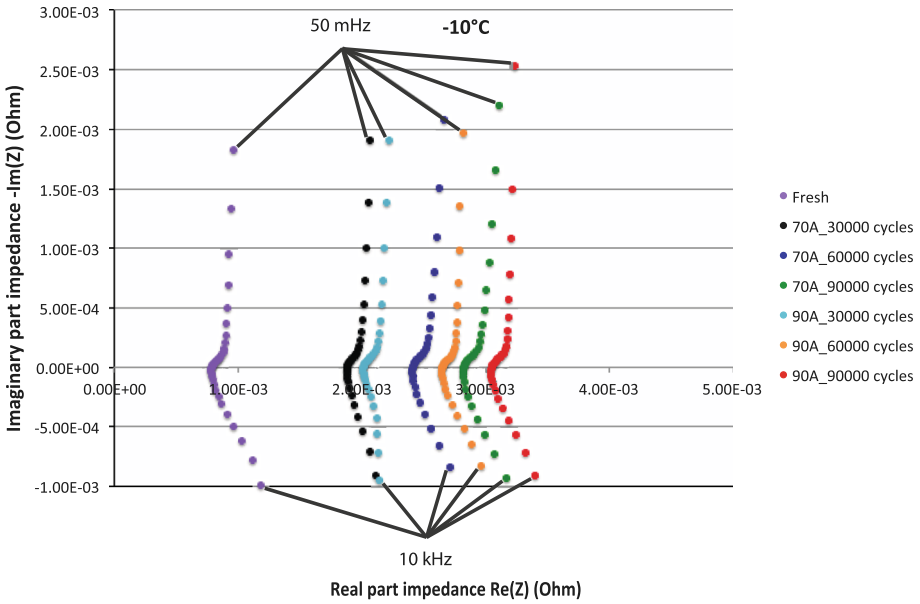

Fig. 18 Effect of the cycle life on the impedance spectra at −10 °C in a Nyquist plot

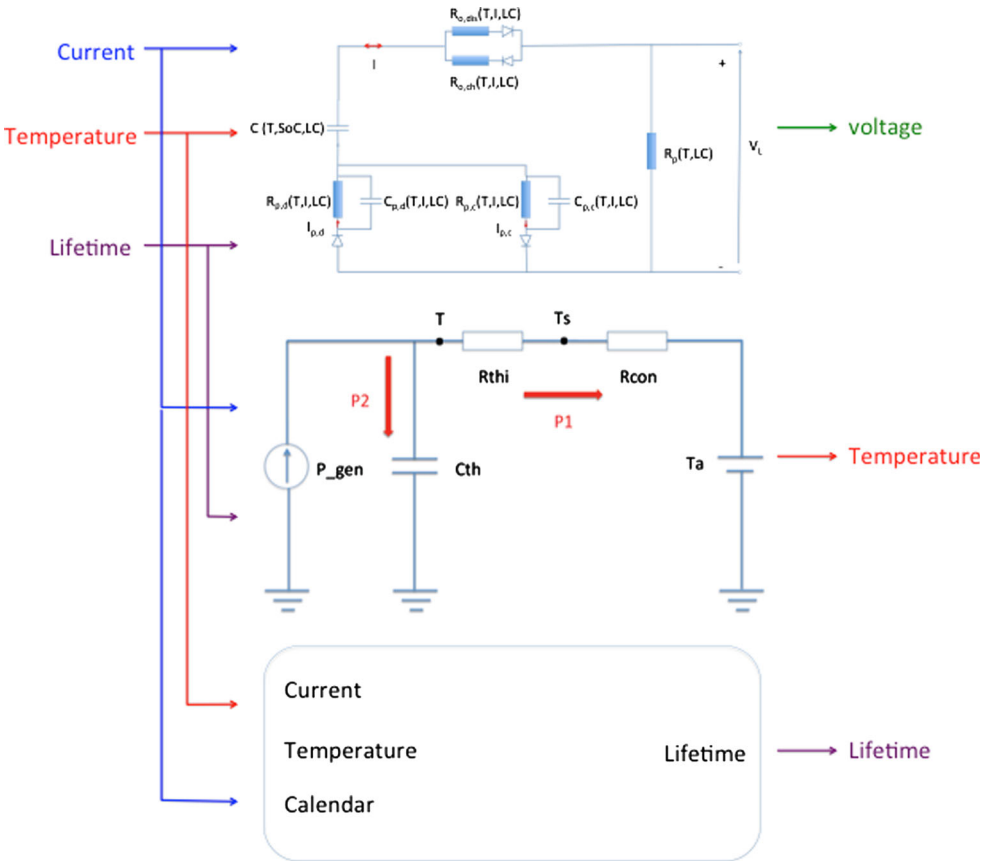

Fig. 19 New EDLC model approach

However, in the Sects. 3.1, 3.2 and 3.3, we have seen that the increase of the internal resistance and decrease of the capacitance of the EDLC is depends on the ambient temperature, current rate and cycle life. Furthermore, in [46, 48, 58–60, 66] it is reported that the ageing of the EDLC also depends of the calendar life.

Therefore, we can conclude that the proposed model is only sufficient in the beginning of lifetime. In order to

predict the behaviour of the EDLC during the long-term, there is a need for a new model approach. In this paper, we propose the model as presented by Fig. 19. The model exists of 3 levels. The first level is the electrical model, which has only electrical parameters such as ohmic resistances and capacitors. The resistances $R_{o,ch}$ and $R_{o,dis}$ represents the ohmic resistances during charging and discharging. While the two RC circuits stand for the polarization behaviour of the EDLC during charge and discharge, while C is the rated capacitance of the cell. The distribution of the EDLC during charge and discharge is to demonstrate the hysteresis as we observed in Figs. 7 and 8.

The second level is the thermal model, where the parameters such as thermal resistance, thermal convection and thermal capacitance are included.

The third level represents the lifetime of the EDLC, whereby the evolutions of calendar and cycling at different conditions are included. These relationships can be extracted at different ways. However, the method based on least-square fitting seems the most interesting path.

In order to simulate the lifetime of the EDLC, there is need for several input parameters such as imposed current, ambient temperature, and cycling voltage conditions.

The use of such model approach has several advantages compared to the existing EDLC models in the literature. Based on this model we will be able to predict the EDLC behaviour during short and long-term. Further, the model will assist us to set up an optimized control strategy for the thermal management, where a long cycle life and high performances can be assured.

4 Conclusions

In this paper, an extended cycle life analysis has been carried out at different ambient temperatures and current rates. The experimental results show that the increase of the internal resistance is significantly higher at temperatures 60 and 40 °C compared to 10 °C. This result is due to the higher increase of the internal resistance, which was, after 110,000 cycles, about 130 and 56 % at 60 and 40 °C, respectively. According to the EIS measurements, the increase of the ageing during cycling is also due to the increase of the imaginary part of the resistance at low frequencies. This indicates the capacitance fade.

Further, the experimental results showed that the hysteresis of the EDLC increases during cycling and that the increase is temperature dependent.

Finally in this paper, a new EDLC model approach is presented to predict the EDLC short term and long-term behaviour.

Acknowledgments We like to thank NESSCAP for the material support of this project in terms of EDLC cells.

References

1. Maggetto G, Van Mierlo J (2001) Mater Fuel Cell Syst 26:9–26
2. Van Mierlo J, Maggetto G, Lataire Ph (2006) Energy Convers Manag 47:2748–2760
3. Van den Bossche P, Vergels F, Van Mierlo J, Matheys J, Van Autenboer W (2005) J Power Sources 162:1277–1282
4. Omar N, Daowd M, Van den Bossche P, Hegazy O, Smekens J, Coosemans Th, Van Mierlo J (2012) Energies 5:2952–2988
5. Mulder G, Omar N, Pauwels N, Meeus M, Leemans F, Verbrugge B, De Nijs W, Van den Bossche P, Six D, Van Mierlo J (2013) Electrochem Acta 87:473–488
6. Omar N, Van Mulders F, Van Mierlo F, Van den Bossche P (2009) J Asian Electr Vehicles 7:1277–1282
7. Abderrahmane H, Emmanuel B (2008) Assessment of real behavior of VHE Energy Storage System in heavy vehicles, In proceedings EET-2008 European Ele-Drive Conference, Geneva, Switzerland, 2008
8. Omar N, Verbrugge B, Van den Bossche P, Van Mierlo J (2010) Electrochem Acta 55:7524–7531
9. Cheng J, Van Mierlo J, Van den Bossche P, Lataire Ph (2006) Super capacitor based energy storage as peak power unit in the applications of hybrid electric vehicles, In proceedings PEMD 2006, Dublin, Ireland, 2006
10. Akli C.R, Roboam X, Sareni B, Jeunesse A (2007) Energy management and sizing of a hybrid locomotive, In Proceedings EPE 2007, Aalbörg, Denmark, 2007
11. Pay S, Baghzouz Y (2003) Effectiveness of battery-supercapacitor combination in electric vehicles, In Proceedings IEEE Power Technology Conference, Bologna, Italy, 2003
12. Wang T, Yu H, Zhu C (2008) Hybrid energy Sources for hybrid electric vehicle propulsion, In Proceedings IEEE Vehicle Power and Propulsion Conference, Harbin, China, 2008
13. Van Mierlo J, Maggetto G, Van den Bossche P (2004) J Power Sources 128:76–89
14. Omar N, Daowd M, Hegazy O, Van den Bossche P, Coosemans Th, Van Mierlo J (2012) Energies 5:4533–4568
15. Kötz R, Carlen M (2000) Electrochem Acta 45:2483–2498
16. Barrero R, Coosemans Th, Van Mierlo J (2009) Hybrid buses: defining the power fow management strategy and energy storage system needs, In Proceedings EVS 24, Stavanger, Norway, 2009
17. Omar N,Van Mulders F, Timmermans J.M, Van Mierlo J, Van den Bossche P, Culcu H (2009) Effectiveness evaluation of a supercapacitor-battery parallel combination for hybrid heavy lift trucks, In proceedings EVS 24, Stavanger, Norway, 2009
18. Van Mulders F, Timmermans J.P, McCaffrey Z, Van Mierlo J, Van den Bossche P (2008) World Electr Vehicle J 2:32–45
19. Abderahmane H, Emmanuel B (2008) Assessment of real behavior of vhe energy storage system in heavy vehicles. In proceedings EET-2008 European Ele-Drive Conference, Brussels, Belgium, 2008
20. Ciccarelli F, Iannuzzi D, Tricoli P (2012) Transp Res C 24:36–49
21. Barrade Ph (2003) Energy storage and applications with supercapacitors, In Proceedings ANE, Bressanone, Italy, 2003
22. Karden E, Ploumen S, Fricke B, Miller T, Snyder K (2007) J Power Sources 168:2–11
23. Van Voorden AM, Elizondo LMR, Paap GC, Verboomen J, Van der Sluis L (2007) The application of super capacitors to relieve battery-storage systems in autonomous renewable energy systems, In Proceedings Power Technology, Lausanne, Switserland, 2007

24. Manwell J, McGowan J (1994) Evaluation of battery models for wind/hybrid power system simulation, In proceedings of the 5th European Wind Energy Association Conference, Thessaloniki, Greece, 1994
25. Rufer A, Barrade P (2002) IEEE Trans Ind Appl 38:1151–1159
26. Platform Ecologische Vlootbeheer http://www.vmx.be/mobimixbe-platform-ecologisch-vlootbeheer Accessed 17 July 2013
27. Auer J, Hipp E, Lexen G (2005) Efficient hybrid drive system with ultracaps for city buses, In proceedings 14th Aachener Koloquium Fahrzeug und Motorentechnik, Aachen, Germany, 2005
28. Schneuwly A (2006) Designing auto power systems with ultracapacitors, In proceedings of Embedded Systems Conference, California, USA, 2006
29. ISE Corporation http://www.isecorp.com/pdfs/energy-storage-system-brochure.pdf Accessed 17 July 2013
30. Kerschl S, Hipp E (2005) Efficient hybrid drive system with ultracaps for city buses, In proceedings 14th Aachener Kolloquium Fahrzeug und Motorentechnk, Aachen, Germany, 2005
31. Barrero R, Tackoen X, Van Mierlo J (2010) J Rail Rapid Transit 224:207–225
32. Steiner M, Scholten J (2005) Energy storage on board of railway vehicles, In Proceedings EPE, Germany, 2005
33. http://www.mobility.siemens.com/mobility/global/Documents/en/railsolutions/ railway-electrification/dc-traction-power-supply/sitras-ses2-en.pdf Accessed 17 July 2013
34. Culcu H, Van Mierlo J, Doorsselaere V, Verstyhe M, Developing a simulation program for Traditional and Hybrid Off-Highway Vehicles: simulation and validation of a 12 ton Forklift Truck, from Report of CHOT-project, submitted to IWT, 1–40
35. Verhaeven E (2005) Ultracapacitors combined with different battery technologies, In proceedings 5th BOOSTCAP Meeting, Germany, 2005
36. Kashani OF (2007), Report on the Meeting of the German Chapter of IEEE/IAS/PELs/IES in Mannheim, In Proceedings IEEE Power Electronics Society newsletter, vol 19, 2007
37. Etxeberria-Otadui I, Rujas I, Bilbao E (2010) Design of a supercapacitor based storage system for improved elevator applications, In proceedings Energy Conversion Congres and Exposition, Atlanta, USA, 2010
38. Marie-Francoise JN, Gualous H, Outbibe R, Berthon A (2005) J Power Sources 143:275–283
39. Shah V.A, Jivanadhar A.J, Maheshwari R, Roy R (2008) Review of ultracapacitor technology and its applications, In proceedings 15th National Power Systems Conference, India, 2008
40. HyHEELS http://cordis.europa.eu/search/index.cfm?fuseaction=proj.document&PJ_RCN=8330998 Accessed on 17 July 2013
41. Chaari R, Briat O, Delétage J.Y, Lallemand R, Kauv J, Coquery G, Vinassa JM (2011) Ageing quantification of supercapacitors during power cycling using online and periodic characterization tests, In proceedings VPPC 2011, Chicago, USA, 2011
42. Hammar A, Venet P, Lallemand R, Coquery G, Rojat G (2010) IEEE Trans Ind Electron 57:3972–3979
43. Uno M, Tanaka K (2012) IEEE Trans Ind Electron 59:4704–4712
44. Bertrand N, Briat O, El Brouji H, Vinassa JM (2010) Impact of the aging of supercapacitors in power cycling on the behaviour of hybrid electric vehicles applications, In proceedings VPPC 2010, Lille, France, 2010
45. Coquery G, Lallemand R, Kauv J, Soucaze-Guillous B, De Monts A, Chabas J, Darnault A (2004) First accelerated ageing cycling test on supercapacitors for transportation applications, In proceedings ESSCAP'2004, Belfort, France, 2004
46. Kötz R, Ruch PW, Cericola D (2010) J Power Sources 195:923–928
47. Oukaour A, Tala-Ighil B, Al Sakka M, Gualous H, Gally R, Boudart B (2013) Electr Power Syst Res 96:330–338
48. Gualous H, Gallay R, Al Sakka M, Oukaour A, Tala-Ighil B, Boudart B (2012) Microelectron Reliab 52:2477–2481
49. Azais P (2003) Recherches des causes du vieillissement de supercondensateurs à électrolyte organique à base de carbones activés, Master thesis. Université d'Orléans, Orléans
50. Azaïs P, Duclaux L, Florian P, Massiot D, Lillo-Rodenas MA, Linares-Solano A, Peres J, Jehoulet C, Béguin F (2007) J Power Sources 171:1046–1053
51. Linzen D, Buller S, Karden E, De Doncker RW (2005) IEEE Trans Ind Appl 41:1135–1141
52. NESSCAP http://www.nesscap.com/product/edlc_large2.jspBio-Logic Accessed 17 July 2013
53. Pec Corporation http://www.peccorp.com/SBT0550-tabs-glance.html Accessed 17 July 2013
54. Bio-Logic http://www.bio-logic.info/ Accessed 17 July 2013
55. IEC62576: Electric double-layer capacitors for use in hybrid electric vehicles: test methods for electrical characteristics, http://shop.bsigroup.com/ProductDetail/?pid=000000000030183420 Accessed 17 July 2013
56. Omar N (2012) Assessment of rechargeable energy storage systems for plug-in hybrid electric vehicles, Ph.D. thesis, Vrije Universiteit Brussel, Brussel, Belgium, 2012
57. Maxwell Boostcap http://www.maxwell.com/ Accessed 17 July 2013
58. Kurzweil P, Chwistek M (2008) J Power Sources 176:555–567
59. Hahn M, Kötz R, Gallay R, Siggel A (2006) Electrochem Acta 52:1709–1712
60. Brouji HE, Briat O, Vinassa JM, Vertrand N, Woirgard E (2008) Ageing quantification of ultracapacitor during calendar life and power cycling tests using a physically-based impedance model, In Proceedings ESSCAP 2008, Rome, Italy, 2008
61. Zubieta L, Bonert R (1998) IEEE Trans Ind Appl 36:1149–1154
62. Zhu M, Weber CJ, Yang Y, Konuma M, Starke U, Kern K, Bittner AM (2008) Carbon 46:1829–1840
63. Bittner AM, Zhu M, Yang Y, Waibel HF, Lonuma M, Starke S, Weber CJ (2013) J Power Sources 203:262–273
64. Omar N, Gualous H, Al Sakka M, Van Mierlo J, Van den Bossche P (2013) electric and thermal characterization of advanced hybrid Li-Ion capacitor rechargeable energy storage system, In Proceedings 4th International Conference on Power Engineering, Energy and Electrical Drives, Istanbul, Turkey, 2013
65. Rafik F, Gualous H, Gallay R, Crausaz A, Berthon A (2006) J Power Sources 165:928–934
66. Bohlen O, Kowal J, Uwe Sauer D (2007) J Power Sources 17:468–475